

# Finite volume analysis of reinforced concrete structure cracking using a thermo-plastic-damage model

B. Selma\*, M. Chekired\*, J. Côté\*, C. Bessette† and L. Jinga†

\* Institut de recherche d'Hydro-Québec  
1800 Lionel Boulet Varennes

† Hydro-Québec  
Réseau de distribution

**Key words:** Crack, damage, OpenFOAM, fvm, plasticity, elasticity, concrete, rheology, temperature

**Abstract** This paper proposes modifications to the phenomenological model formulation called CDPM2, developed by Grassl et al. [1]. The proposed modifications are designed to enhance model performance with coupling to temperature effects. A very strong coupling between nonlinear elasticity, plasticity, nonlocal damage evolution and temperature gradient is used to simulate arbitrary crack propagation. The use of FVM to model solid damage is a numerical challenge. This approach presents some advantages such as: ensuring that discretization is conservative even when the geometry is changing; providing a simple formulation that can be obtained directly from a difference method; and employing unstructured meshes. Most authors have neglected the nonlinearity of concrete in the elastic domain from the start of loading to the plastic domain. In this paper we confirm that concrete rheology is not linear even under low loading. Also, since the so-called fracture energy is a key parameter needed to determine the size of cracks and how they propagate in space, we consider that the fracture energy is both material and geometrical parameter dependent. For this reason, we developed a new approach which includes adaptive mesh, nonlinear rheology and thermal effects to re-calculate fracture energy at each time step. Many authors use a constant value obtained from experiments to calculate fracture energy; others use a numerical correlation. In this study, the fracture energy parameter is not constant and can vary with temperature or/and with a change in geometry due to concrete failure. As is well known, the mesh quality of complex geometries is very important for making accurate predictions. A new meshing tool was developed using the C++ programming language. This tool is faster, more accurate and produces a high-quality structured mesh. The predictions obtained were compared to a wide variety of experimental data and showed good agreement.

## 1. Introduction

Concrete is difficult to model because of its quasi-fragility, heterogeneity, porosity and thermal dilation. The literature contains several constitutive models developed to simulate crack formation and propagation. Among them is CDPM2, developed by Grassl et al. [1], which combines damage mechanics and plasticity theory in order to analyze the failure of concrete structures. In the present study, the concept of inelasticity is used instead of plasticity. Inelasticity is close to reality and contains the plastic, elastic and thermal strains, as well as strains due to the effect of time, such as creep. Concrete degradation models are based on the concept of damage, which is often formulated on the basis of mechanical tests on a macro level. However, damage is only one physical parameter and cannot adequately represent crack behavior and random propagation. Crack behavior depends mainly on the damage, crack number and size, mechanical and thermal loading, the initial concrete mix, its age, and the dimensions of the structure. To date, no constitutive models have included all these parameters in the formulation of the damage variable.

In theory, concrete stress has two main causes: damage (highly solicited zones, cracks, microcracks, coalescence problems, aggregate segregation) and plasticity, a mechanism that

is not well understood, especially since plasticity theory was developed from models applied to hyper elastic materials such as plastic and metal. Damage and plasticity are described by continuum mechanics, and their coupling is necessary for concrete degradation modeling. When the thermal gradient is added, the coupling becomes more complex in terms of the discretization of differential equations using, for example, the finite-element method. In the present study, an open-source tool based on the finite-volume method was developed by integrating an algorithm for solving a set of mathematical equations. This tool, coded in OpenFOAM, is in the form of a solver that uses a new library developed specifically for concrete degradation problems.

The finite volume method, recommended by Fryer et al. [2], Demirdzic and Muzaferija [3], Ivankovic et al. [4], Maneeratana [5], and Tukovic et al. [6] for problems related to solid mechanics, was used in the present study to discretize the calculation domain and differential equations. It was chosen because of the complexity of the problem, i.e., the appearance of cracks, their random propagation and the subsequent damage to the structure. Originally developed for fluid mechanics, the finite-volume method has been adapted, with several modifications, to solid mechanics. The work of Menétrey [7]; Grassl et al. [8] and Cervenka and Papanikolaou [9] explains plasticity models based on stress and fracture mechanics. However, as shown in testing, plasticity models are not capable of representing the material's loss of rigidity after cracking. Other researchers, in particular Mazars [10,11]; Grassl and Jirasek [12]; Cicekli et al. [14]; Voyiadjis et al. [13]; and Grassl et al. [1,8], have combined plasticity models with damage mechanics. The present study is based mainly on the work of Grassl et al. [1]. This model is complete enough to be applied to cases involving lower loads (compression or traction) while considering isotropic damage during the deformation process. The damage model, used by Grassl and Jirasek [12], is based on a single parameter for both load types (compression and traction). Those authors nevertheless recognized that their model was inadequate for dealing with a deformation following biaxial compression-traction tests, and recommended using other damage models with several parameters. Recently, Grassl et al. [8] used the model known as CPDM1 (Concrete Plasticity Damage Model 1) to develop an improved version by adding a two-parameter isotropic damage model. In the present work, a damage law was developed based on the work of Mazars [10, 11] and Oliver et al. [15].

## 2. Mathematical modeling

The general formulation for elasto-plastic with damage is written as follows:

$$\dot{\sigma} = (1 - \mathbf{d})\dot{\bar{\sigma}} = (1 - \mathbf{d})\mathbf{D}_e: (\dot{\epsilon} - \dot{\epsilon}_p) \quad (1)$$

Where  $\dot{\sigma}$  and  $\dot{\bar{\sigma}}$  represent the total and effective stresses, respectively, and  $(\mathbf{d})$  is the isotropic damage variable ( $\mathbf{d}=\mathbf{0}$ : healthy structure;  $\mathbf{d}=\mathbf{1}$ : damaged structure). In OpenFOAM,  $\mathbf{d}$  is written as follows:

$$\mathbf{d} = d[\text{cell}] \quad (2)$$

The term “cell” defines the index of a finite volume in the mesh. Effective stress is expressed by the following equation:

$$\bar{\sigma} = \mathbf{D}_e: (\epsilon - \epsilon_p) \quad (3)$$

The terms  $(\dot{\epsilon})$  and  $(\dot{\epsilon}_p)$  represent the total and plastic deformation rates, respectively. Plastic deformation,  $\dot{\epsilon}_p$ , is determined using the concept of plasticity governed by a set of equations and conditions, as follows:

$$\dot{\epsilon} = \dot{\epsilon}_e + \dot{\epsilon}_p, \bar{\sigma} = E\dot{\epsilon}_e, \dot{\epsilon}_p = \dot{\lambda}_p m(\bar{\sigma}, \kappa_p), \dot{\kappa}_p = \frac{\dot{\lambda}_p m}{\dot{\kappa}_h(\bar{\sigma})} (2\cos\bar{\theta})^2 \quad (4)$$

Where  $E$  is the initial Young modulus,  $m(\bar{\sigma}, \kappa_p)$  represents the plastic flow vector, and  $\dot{\lambda}_p$  is the plastic multiplier rate calculated under the following conditions:

$$F_p(\bar{\sigma}, \kappa_p) \leq 0, \quad \dot{\lambda}_p \geq 0, \quad \text{et} \quad \dot{\lambda}_p F_p(\bar{\sigma}, \kappa_p) = 0 \quad (5)$$

### 2.1 Failure interface function

Function  $F_p(\bar{\sigma}, \kappa_p)$  defines the failure interface, which is a line separating the elastic domain and the cracked area.

$$F_p(\bar{\sigma}, \kappa_p) = \left\{ [1 - q_{h1}] \left( \frac{\bar{p}}{\sqrt{6}f_c} + \frac{\bar{\sigma}_V}{f_c} \right)^2 + \sqrt{\frac{3}{2}} \frac{\bar{p}}{f_c} \right\}^2 + m_0 q_{h1}^2(\kappa_p) q_{h2}(\kappa_p) \left[ \frac{\bar{p}}{\sqrt{6}f_c} r(\cos\bar{\theta}) + \frac{\bar{\sigma}_V}{f_c} \right] - q_{h1}^2(\kappa_p) q_{h2}^2(\kappa_p) \quad (6)$$

With  $\bar{\sigma}_V = \frac{1}{3} tr(\sigma)$

The work of Grassl et al. [1] provides more detail about the CDPM2 model.

### 2.2 Concrete elasticity

Figure 2 shows the change in the Poisson coefficient and Young modulus based on the work of Ottosen [16]:

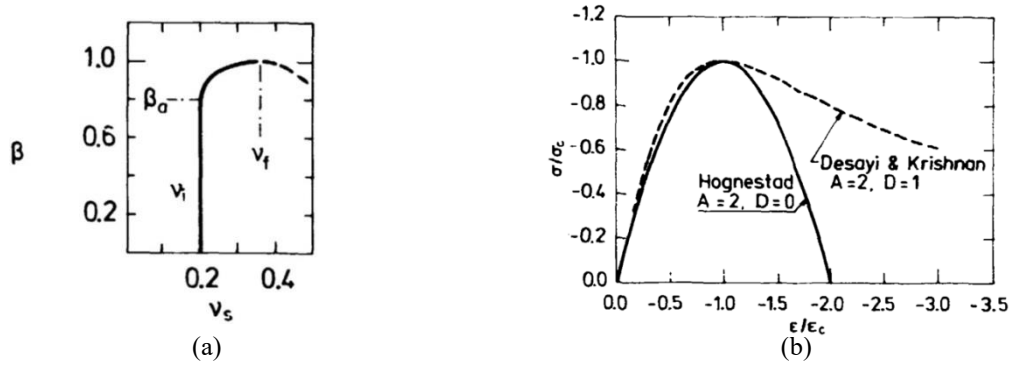


**Figure 1** : Change in rheological properties of concrete: (a) Poisson coefficient (b) Influence of parameters A and B (Ottosen [16])

L'évolution du coefficient de Poisson,  $\nu$ , est donnée par la relation suivante:

$$\nu = \begin{cases} \nu_0 & \text{si } \beta \leq \beta_0 \\ \nu_f - (\nu_f - \nu_0) \sqrt{1 - \left( \frac{\beta - \beta_0}{1 - \beta_0} \right)^2} & \text{si } \beta > \beta_0 \end{cases} \quad (7)$$

For any type of concrete or load  $\nu_f = 0.36$  and  $\beta_0 = 0.8$ . Parameter  $\nu_0$  represents the initial Poisson coefficient. Variable  $\beta$  defines the ratio of the equivalent stress over the compression withstand limit:

$$\beta = \frac{\epsilon_{eq}}{f_c'} \quad (8)$$

Absence of a load ( $\epsilon_{eq} = 0$ ) implies that  $\beta = 0$ , and only in that case is the concrete response considered elastic-linear. The variation in the elasticity modulus is expressed by the following non-linear equation:

$$E_{nl} = \frac{1}{2} E_0 - \beta \left( \frac{1}{2} E_0 - E_f \right) + \sqrt{\left[ \frac{1}{2} E_0 - \beta \left( \frac{1}{2} E_0 - E_f \right) \right]^2 - \beta E_f^2 [A(1 - \beta) - 1]} \quad (9)$$

If  $\beta = 0$ , equation (33) will give:  $E_{nl} = E_0$  (linear response).

The term  $E_f$  represents the Young modulus at the fracture point, and is defined as follows:

$$E_f = \frac{E_0}{1+4(B-1)\left(\frac{\sqrt{J_2}-1}{f_c \sqrt{3}}\right)} \quad (10)$$

A and B are parameters of the model (A=1 and B=2 according to Desayi and Krishnan [17]).  $f_c$  is the compression withstand limit, and  $J_2$  represents the plasticity criterion defined by:

$$J_2 = \frac{1}{3}(I_1^2 - 3I_2) \quad (11)$$

### 2.3 Concrete plasticity

The deformations resulting from mechanical loading are shown in Figure 3.

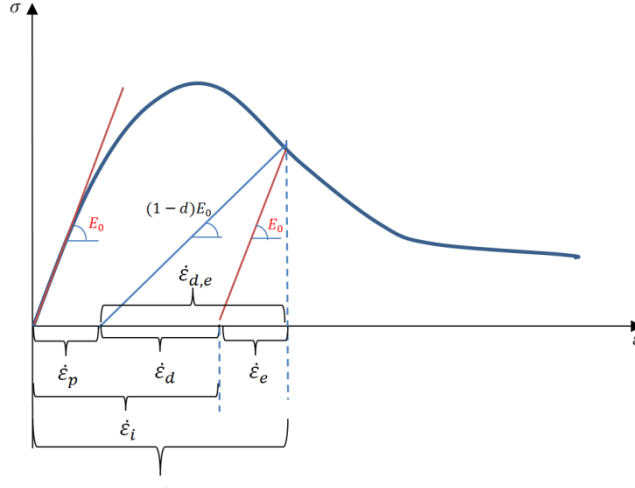


**Figure 3:** Change in concrete deformation under compression

It can be seen that there are several mathematical formulations in terms of equivalent deformations and in the form of increments for small displacements:

$$\dot{\varepsilon} = \dot{\varepsilon}_e + \dot{\varepsilon}_i \quad (12)$$

$$\dot{\varepsilon}_i = \dot{\varepsilon}_p + \dot{\varepsilon}_d \quad (13)$$

$\dot{\varepsilon}_i$  is the increment of inelastic deformation;  $\dot{\varepsilon}_d$  is the increment of deformation due to elasto-plastic damage. In analyzing concrete structure performance, the use of inelastic deformation is the approach closest to reality. Based on Figure 3, deformation due to elasto-plastic damage can be defined. This new parameter is expressed by the following equation:

$$\dot{\varepsilon}_d = \dot{\varepsilon}_{d,e} - \dot{\varepsilon}_e \quad (14)$$

With  $\dot{\varepsilon}_{d,e} = \frac{1}{(1-d)} \dot{\varepsilon}_e$

$\dot{\varepsilon}_{d,e}$  define the deformation after concrete damage while remaining in its elastic domain.

Finally, Equations (13) and (14) give this result:

$$\dot{\varepsilon}_d = \frac{d}{(1-d)} \dot{\varepsilon}_e \quad (15)$$

By definition, elastic deformation is given by the following equation:

$$\dot{\varepsilon}_e = \frac{\dot{\sigma}}{E_0} \quad (16)$$

The increment of total stress is expressed as a function of inelastic deformation, as follows:

$$\dot{\sigma} = 2\mu(\dot{\varepsilon} - \dot{\varepsilon}_i - \dot{\varepsilon}_T) + \lambda \text{tr}(\dot{\varepsilon}) \quad (17)$$

Parameters  $\mu$  and  $\lambda$  are the Lamé coefficients, defined by the following equations:

$$\begin{cases} \mu = \frac{E}{2(1+\nu)} \\ \lambda = \frac{\nu E}{(1+\nu)(1-2\nu)} \end{cases} \quad (18)$$

Consequently, Equations (12), (14) and (15) give the following analytical solution:

$$\dot{\epsilon}_p = \dot{\epsilon} - \frac{1}{1-d} \dot{\epsilon}_e \quad (19)$$

Equations (12) to (19) are expressed in terms of equivalent deformations in order to calculate the equivalent plastic deformation, which is approximately equal to the plastic multiplier  $\dot{\lambda}_p$ . The following equation may therefore be concluded:

$$\dot{\epsilon}_{eq}^p \cong \dot{\lambda}_p \quad (20)$$

Equations (4) and (20) therefore yield this equivalence:

$$\dot{\epsilon}^p = \dot{\epsilon}_{eq}^p m(\bar{\sigma}, \kappa_p) \quad (21)$$

The plastic normal (or plastic flow vector),  $m(\bar{\sigma}, \kappa_p)$ , is defined by:

$$m(\bar{\sigma}, \kappa_p) = \frac{\partial}{\partial \bar{\sigma}} G_p(\bar{\sigma}, \kappa_p) \quad (22)$$

#### 2.4 Influence of temperature on concrete degradation

Temperature variations affect rheological parameters ( $E$ ,  $f_t$ , and  $f_c$ ) as well as the dilation coefficient and thermal conductivity. In this study, the correlations established by Shoukry et al. [23] were incorporated into the numerical tool as follows:

$$f_t(T) = 0.55 \sqrt{\dot{f}_t} - 0.018(T - 20), \quad f_c(T) = \dot{f}_c - 0.13(T - 20) \quad \text{and} \quad E(T) = E_0 - 0.10627(T - 20)$$

The concrete dilation coefficient was assumed to be fixed at  $\alpha = 6.8 \times 10^{-6} \text{ 1/C}^\circ$  according to ACI (2019). The rheological parameters are in MPa for ( $f_t$ ,  $f_c$ ) and in GPa for Young's modulus. To determine thermal conductivity, the model of Kim et al. [24] was used.

$$k_c = k_0 [0.293 + 1.01V_g] \left[ 0.8 \left( 1.62 - 1.54 \left( \frac{w}{c} \right) \right) + 0.2R_h \right] \times [1.05 - 0.0025T] [0.86 + 0.0036V_s] \quad (23)$$

Where  $k_0$  is the reference conductivity of concrete (at  $T=20\text{C}^\circ$ ),  $V_g$  the volume fraction of the large aggregate, ( $w/c$ ) the water/cement ratio,  $R_h$  the humidity and  $V_s$  the volume fraction of the sand. Thermal damage is calculated according to the following correlation, Jirasek and Bazant [25]:

$$D^T = 1 - (0.03931 + \exp(-0.002T)) \quad (24)$$

Equation (24) does not take elastic or plastic deformation into account. This equation is used to correct mechanical damage, as follows:

$$D_{global} = (1 - D^M)(1 - D^T) \quad (25)$$

#### 2.5 Analytical solution proposed to determine plastic deformation

The iterative algorithms proposed in the literature [11,12,27] to calculate the plastic multiplier and deduce the plastic deformation have a number of disadvantages, including high effort calculation and high residuals. The contribution of the present study is of a theoretical nature; it is based on a mathematical development for determining plastic deformation. For concrete, the inelastic definition is used, in which plastic deformation is implicitly included. Figure 3 shows the definition of each variable in terms of stress-deformation curve. Moreover, the following condition was developed and verified:

$$\frac{1}{2} \dot{\epsilon} \leq \dot{\epsilon}_p \leq \dot{\epsilon} \quad (26)$$

Thus, based on the following equations:

$$E_p = (1 - d)E \quad (27)$$

And

$$\dot{\varepsilon} = \dot{\varepsilon}_e + \dot{\varepsilon}_p \quad (28)$$

Using the total stress rate applied as follows:

$$\frac{\dot{\sigma}}{E_{ep}} = \frac{\dot{\sigma}}{E} + \frac{\dot{\sigma}}{E_p} \quad (29)$$

From Equation (29) it may be deduced that:

$$E_{ep} = \frac{EE_p}{E+E_p} \quad (30)$$

Given that:

$$E_{ep} = \frac{\dot{\sigma}}{\dot{\varepsilon}} \quad (31)$$

Equations (27) and (30) give:

$$\dot{\varepsilon}_p = \frac{E}{E+E_p} \dot{\varepsilon} \quad (32)$$

By combining Equations (27) and (32), the following result was obtained:

$$\dot{\varepsilon}_p = \frac{1}{2-d} \dot{\varepsilon} \quad (33)$$

Using extreme conditions of damage, the following system is found:

$$\begin{cases} \dot{\varepsilon}_p = \frac{1}{2} \dot{\varepsilon} & \text{si } d = 0 \\ \dot{\varepsilon}_p = \dot{\varepsilon} & \text{si } d = 1 \end{cases} \quad (34)$$

Based on equation system (34), it may be deduced that the following equation is true at all times:

$$\frac{1}{2} \dot{\varepsilon} \leq \dot{\varepsilon}_p \leq \dot{\varepsilon} \quad (35)$$

This new condition was implemented into the numerical toolbox developed in the present study. Computational stability and convergence are observed during simulation.

## 2.6 Components of damaged concrete

Mazars' two damage laws [10,11], in their original and modified versions, have been widely used in the study of concrete degradation. In the present work, an exponential law was incorporated into the numerical code (please see those studies for more details). Mathematically, Mazars' laws have exponential form; however, in this model, the exponential law is written explicitly as follows:

$$\mathbf{d}_t = 1 - \exp\left(-\frac{\varepsilon_{eq,t}}{\varepsilon_f}\right) \quad (36)$$

$$\mathbf{d}_c = 1 - \exp\left(-\frac{\varepsilon_{eq,c}}{\varepsilon_f}\right) \quad (37)$$

This new formulation makes implicit use of fracture energy in the term  $\varepsilon_f = G_f / (f_t h_e)$ . Mazars' laws do not use this important parameter, considered to be both a physical and geometric property of the material. The overall damage rate is given by the same equation as the one developed by Mazars [10]:

$$\mathbf{D} = \alpha_t \mathbf{d}_t + (1 - \alpha_t) \mathbf{d}_c \quad (38)$$

The present work uses the following equation from Grassl et al. [1]:

$$\alpha_c = \sum_{i=1}^3 \frac{\bar{\sigma}_{c,i}(\bar{\sigma}_{t,i} + \bar{\sigma}_{c,i})}{\|\bar{\sigma}_p\|^2} \quad (39)$$

Where

$$\alpha_t = (1 - \alpha_c); \varepsilon_{eq,t} = \sqrt{\sum_i^3 < \varepsilon_i >_+^2}; \varepsilon_{eq,c} = \sqrt{\sum_i^3 < \varepsilon_i >_-^2}; \bar{\sigma}_p = \frac{1}{3} tr(\bar{\sigma}) \bar{\sigma}_{t,i} = < \bar{\sigma}_i >_+; \bar{\sigma}_{c,i} = < \bar{\sigma}_i >_-$$

Equations (36) and (37) are based on the work of Oliver et al. [53], whose model had limits in terms of biaxial and shear loading. Equivalent deformation is uniform, whether for mode I or mode II. The concept of this development is based on the use of Mazars' laws [10,11], because of their advantages in biaxial tests, and on the exponential law of Oliver et al. [53], which includes fracture energy. Combining these two laws yielded Equations (36) and (37).

### 2.9 Cohesive forces on the concrete-concrete interface

According to Xu and Needleman [18], normal and tangential cohesive forces are expressed as follows:

Normal traction:

$$T_n = -\frac{\Phi_n}{\delta_n} \exp\left(-\frac{\Delta_n}{\delta_n}\right) \left\{ \frac{\Delta_n}{\delta_n} \exp\left(-\frac{\Delta_t^2}{\delta_t^2}\right) + \frac{1-q}{r-1} \left[1 - \exp\left(-\frac{\Delta_t^2}{\delta_t^2}\right)\right] \left[r - \frac{\Delta_n}{\delta_n}\right] \right\} \quad (40)$$

Tangential traction :

$$T_t = -\frac{\Phi_n}{\delta_n} \left(2 \frac{\delta_n}{\delta_t}\right) \frac{\Delta_t}{\delta_t} \left\{ q + \left(\frac{r-q}{r-1}\right) \frac{\Delta_n}{\delta_n} \right\} \exp\left(-\frac{\Delta_n}{\delta_n}\right) \exp\left(-\frac{\Delta_t^2}{\delta_t^2}\right) \quad (41)$$

The parameters are defined in Xu and Needleman [18]. However, the characteristic lengths,  $\delta_n$  and  $\delta_t$ , were determined using the equation proposed by Hillerborg et al. [19]:

$$\delta_n = \delta_t = \frac{G_f E}{f_t^2} \quad (42)$$

$G_f$  is the fracture energy expressed by the equation of Bazant and Becq-Giraudon [26]:

$$G_f = (0.0469h_e^2 - 0.5h_e + 26)f_c^{0.7} \quad (43)$$

### 2.10 Estimation of crack opening

Based on the work of Bazant and Oh [27], crack thickness is expressed as follows:

$$w_c = l_{ch} \varepsilon_c \quad (44)$$

$l_{ch}$  is the characteristic length defined by Equation (42), and  $\varepsilon_c$  is the deformation in the crack area. By combining Equations (42) and (44):

$$w_c = \frac{G_f E}{f_t^2} \varepsilon_c \quad (45)$$

It should be noted that in the present work, the term  $\varepsilon_c$  has been replaced by equivalent deformation,  $\tilde{\varepsilon}$ , because of its involvement in the damage parameter calculation. In addition, crack thickness is proportional to equivalent deformation. The following equation was developed and incorporated into the numerical tool:  $w_c = \frac{G_f E}{f_t^2} \tilde{\varepsilon}$

## 3. Development of an open-source toolbox for concrete cracking

As part of this study, a meshing tool was developed. The mesh generated contained two main volume types: hexahedron and prism. Table 1 provides some of the mesh characteristics in the case of beam.

**Table 1:** Mesh generation and characteristics

| Geometry (cm)               | Number of FVs         | Type of mesh                | Time (s) | Max. Skewness | Max. aspect ratio |
|-----------------------------|-----------------------|-----------------------------|----------|---------------|-------------------|
| Beam 20(W) × 40(H) × 420(L) | 0.9 × 10 <sup>6</sup> | Hex. (96.5%) / Prism (4.5%) | 32       | 0.78          | 7.95              |

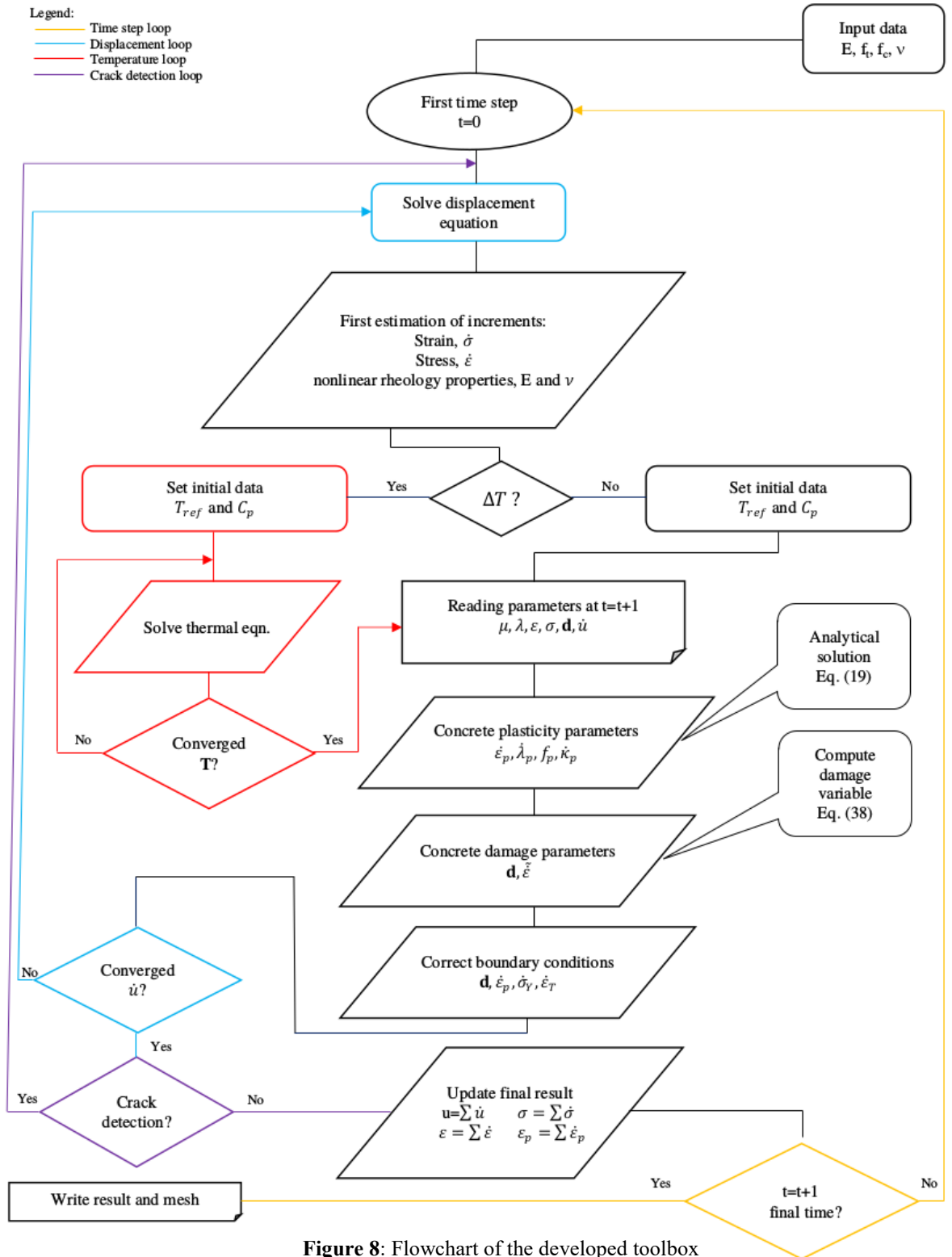


Figure 8: Flowchart of the developed toolbox

#### 4. Experimental validation

To assess the validity of the proposals developed in this work, the numerical simulation results were compared with lab test results. In this way, the model’s ability to reliably predict the response of reinforced concrete to various types of loading was determined. The experimental results used for the validation were those of Kupfer et al. [28] in Figures 11 and 12, of Nooru [20] in Figure 13, of Imran [21] in Figure 14, and of Mirzazadeh and Green [22] in Figure 15. It can be seen that the model’s results are very similar to those obtained experimentally, regardless of the type of loading the concrete samples were subjected to.



### 4.1 Kupfer's biaxial tests

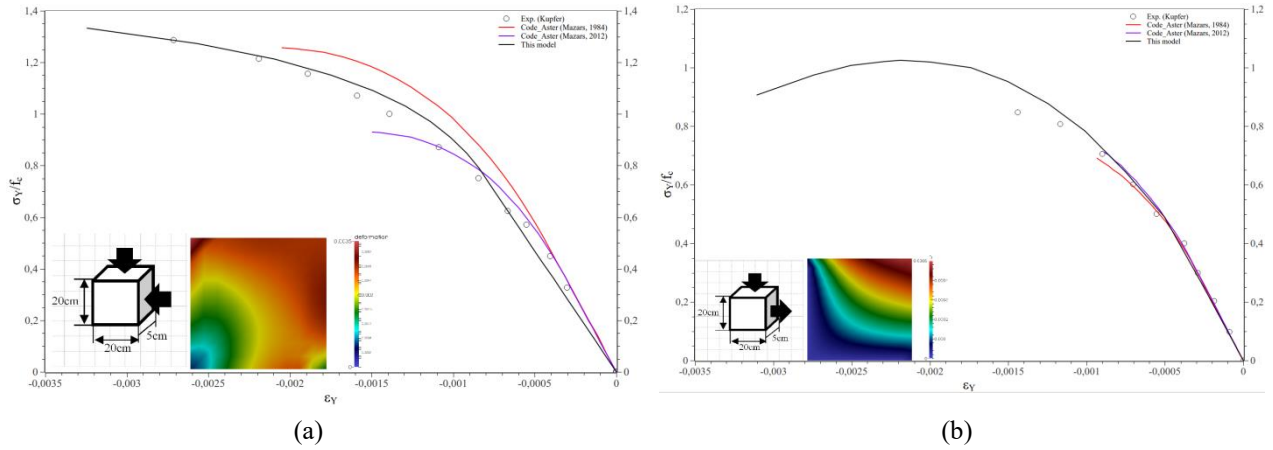


**Figure 11:** Comparison between experimental result and model (a) Biaxial compression (b) Compression-Traction

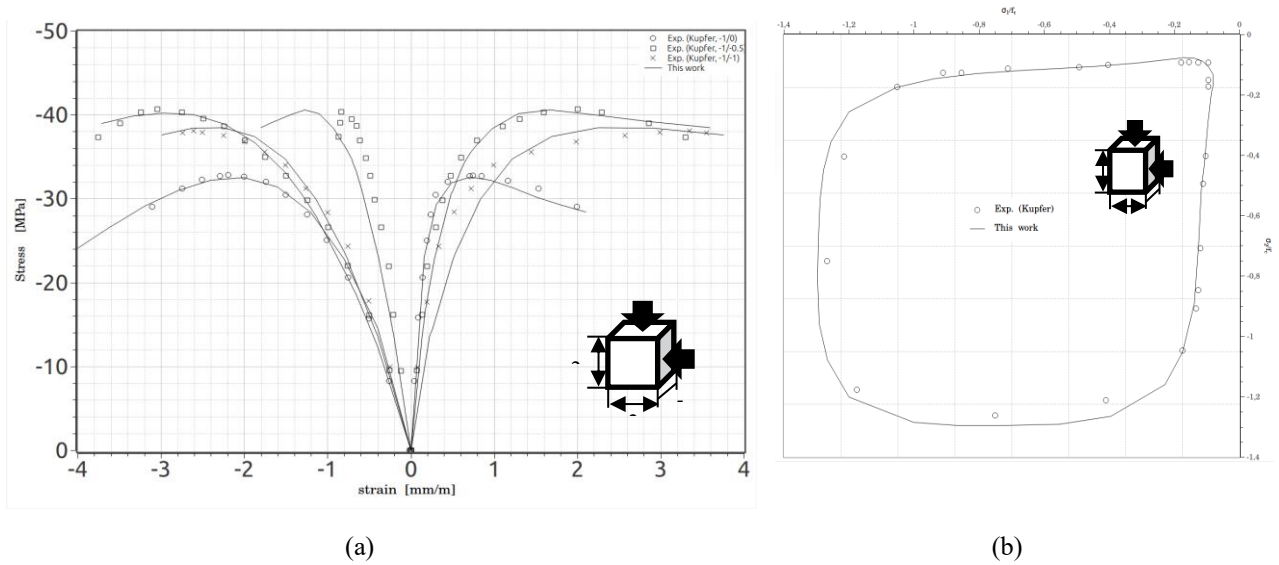


**Figure 12:** (a) Uniaxial and biaxial compression (b) Biaxial compression: Axial deformations

### 4.2 Nooru's shear tests

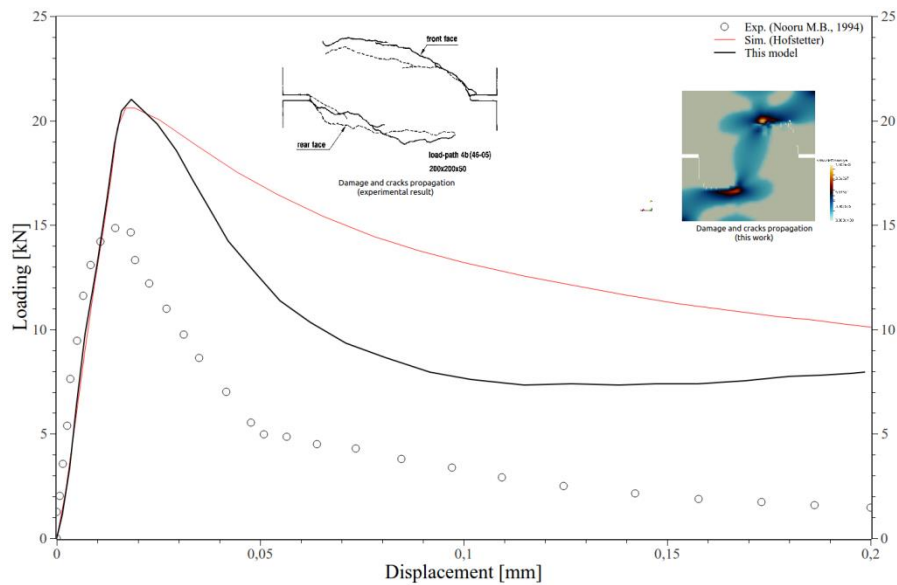


**Figure 13:** Nooru-Mohamed's shear tests [20] and numerical result

### 4.3 Imran's confinement tests

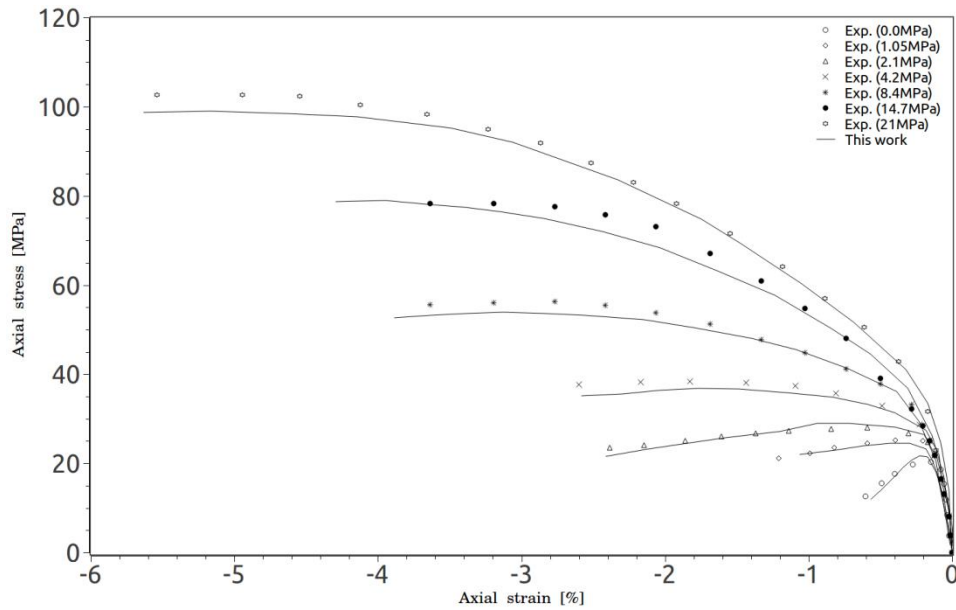


Figure 14: Confinement test on saturated concrete with  $E/C=0.75$

### 4.4 Mirzazadeh and Green four-point beam [22]

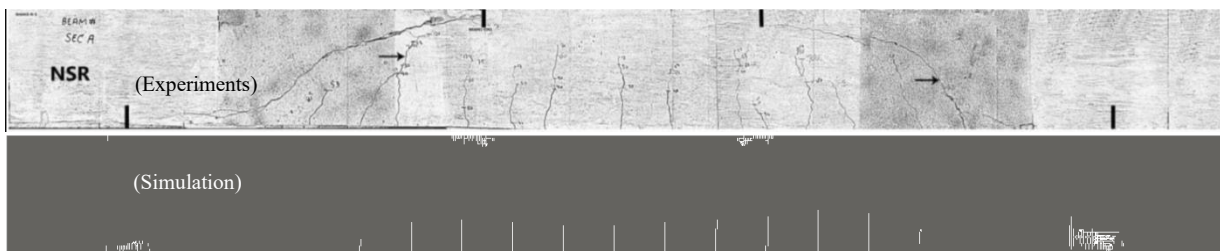


Figure 15: Beams with no stirrups (average temperature inside beam:  $30\text{C}^\circ$ )

## 6. Conclusion

The proposals developed were validated based on experimental results obtained from the literature. The mathematical model resulting from the present work may be considered generic and scalable for the study of concrete degradation. The model also takes into account concrete expansion due to thermal gradient. The effect of fracture energy on fracture behavior is considered to be the most important factor. A number of nonlinear laws and analytical solutions were introduced with the aim of simulating concrete response to cracking but also to reduce calculation effort. The following points were noted during the numerical simulations performed by means of parallel calculations:

- The damage variable has more influence on cracks in compression mode than in strain mode.
- Plastic deformations have a considerable effect on crack direction and opening.
- Plastic deformations are more numerous in mode I (strain) than mode II (compression).
- Nonlinear response was observed in the elastic part (see Kupfer's biaxial tests).
- The degradation of the concrete's Young modulus starts well before its compression or traction withstand limit.
- The following equation applied at all times, regardless of the type of loading:

$$\frac{1}{2}\dot{\epsilon} \leq \dot{\epsilon}_p \leq \dot{\epsilon}$$

- Fracture energy depends on geometry, coarse aggregate size and the material's rheological properties.
- Some of the samples had gouges in them, which accelerated the appearance of cracking.
- Crack thickness is strongly influenced by fracture energy.
- The cohesive forces at the concrete-concrete interface depend on the fracture energy. Consequently, the fracture energy value determines whether or not new cracked surfaces will form.

### References:

- [1] Grassl P., Xenos D., Nystrom U., Rempling R., and Gylltoft K. *CDPM2: A damage-plasticity approach to modelling the failure*. International Journal of Solids and Structures, Vol. 50, pp. 3805-3816 (2013)
- [2] Fryer Y.D., Bailey C., Cross M., and Lai C.H. *A control volume procedure for solving the elastic stress-strain equations on an unstructured mesh*. Appl. Math. Modelling, vol. 15, pp. 639-645 (1991)
- [3] Demirdzic I. and Muzaferija S. *Finite volume method for stress analysis in complex domains*. International Journal for numerical Methods in Engineering, vol. 37, pp. 3751-3766 (1994)
- [4] Ivankovic A., Demirdzic I., Williams J.G., and Leever P.S. *Application of the finite volume method to the analysis of dynamic fracture problems*. International Journal of Fracture, vol. 66, pp. 357-371 (1994)
- [5] Maneeratana K. *Development of the finite volume method for non-linear structural applications*. Thesis, Imperial College, University of London (2000)
- [6] Tukovic Z., Ivankovic A., and Karac A. *Finite-volume stress analysis in multi-materials linear elastic body*. International Journal for Numerical Methods in Engineering, vol. 93, pp. 400-419 (2013)
- [7] Menétrey Philippe. *Numerical analysis of punching failure in reinforced concrete structures*. Thèse doctorat, École Polytechnique Fédérale de Lausanne EPFL, 1994
- [8] Grassl P., Lundgren K., and Gylltoft K. *Concrete in compression: a plasticity theory with a novel hardening law*. International Journal of Solids and Structures, Vol. 39, pp 5205–5223 (2002)
- [9] Cervenka, J., Papanikolaou, V. *Three-dimensional combined fracture-plastic material model for concrete*. Int. J. of Plasticity, Vol. 24, 12, 2008, ISSN 0749-6419, pp. 2192-2220
- [10] Mazars J. *Application de la mécanique de l'endommagement au comportement non-linéaire et à la rupture du béton de structure*. Thèse de doctorat d'état, Université Paris VI, France (1984)
- [11] Mazars J., Hamon F., Grange S. *A new 3D damage model for concrete under monotonic, cyclic and dynamic loadings*. Materials and Structures, 2014 (on line, DOI 10.1617/s11527-014-0439-8)
- [12] Grassl P. and Jirasek. *Damage-plastic model for concrete failure*. International Journal of Solids and Structures, Vol. 43, pp. 7166-7196 (2006)
- [13] Voyiadjis G.Z., Taqieddine Z.N., and Kattan P.I. *Anisotropic damage-plasticity model for concrete*. International Journal of Plasticity, Vol. 24, pp. 1946-1965, 2008

- [14] Cicekli U., Voyiadjis G.Z., and Abu Al-Rub R.K. *A plasticity and anisotropic damage model for plain concrete*. International Journal of Plasticity, Vol. 23, pp. 1874-1900, 2007
- [15] Oliver J., Cervera M., Oller S., and Lubliner J. *Isotropic damage models and smeared crack analysis of concrete*. In. Computer Aided Analysis and Design of Concrete Structures, Bicanic N, Mang H (eds), Pineridge Press: Swansea, UK, pp. 945-957 (1990)
- [16] Ottosen N.S. *Nonlinear Finite Element Analysis of Concrete Structures*. Risø National Laboratory, DK 4000, Roskilde, Denmark
- [17] Desayi, P. and Krishnan, S. (1964). *Equation for the Stress-Strain Curve of Concrete*. Proc. American Concrete Institute ACI, Vol. 61, 345-350.
- [18] Xu X.-P and Needleman A. *Numerical simulations of fast crack growth in brittle solids*. J. Mech. Phys. Solids, Vol. 42, No. 9, pp. 1397-1434, 1994
- [19] Hillerborg A., Modéer M. and Petersson P-E. *Analysis of crack formation and crack growth in concrete by means of fracture mechanics and finite elements*. Cement and Concrete Research, Vol. 6, pp. 773-782, 1976
- [20] Nooru-Mohamed M.B. *Mixed-mode fracture of concrete: an experimental approach*. Thesis, Delft University of technology, Netherlands (1994)
- [21] Imran I. and Pantazopoulou S.J. Experimental study of plain concrete under triaxial stress. ACI Materials Journal, Vol. 93, No. 6, 1996
- [22] Mirzazadeh M.M. and Green M.F. Non-linear finite element analysis of reinforced concrete beams with temperature differentials, Engineering Structures, Vol. 152 (2017), pp. 920-933
- [23] Shoukry S.N., William G.W., Downie B. and Riad M.Y. *Effect of moisture and temperature on the mechanical properties of concrete*. Construction and Building Materials, Vol. 25, pp. 688-696, 2011
- [24] Kim K.-H, Jeon S.-E, Kim J.-K and Yang S. *An experimental study on thermal conductivity of concrete*. Cement and Concrete Research, Vol. 33, pp. 363-371, 2003
- [25] Jirasek M., and Bazant Z.P. *Inelastic analysis of structures*. John Wiley, ISBN 0-471-98716-6 (2002)
- [26] Bazant Z.P. and Becq-Giraudon E. *Statistical prediction of fracture parameters of concrete and implications for choice of testing standard*. Cement and Concrete Research, Vol. 32, pp. 529–556 (2002)
- [27] Bazant Z.P. and Oh B.H. *Crack band theory for fracture of concrete*. Materials and Structures, Vol. 16, pp. 155-177 (1983)
- [28] Kupfer H., Hilsdorf H.K., and Rusch H. *Behavior of concrete under biaxial stresses*. ACI Journal, vol. 66, pp. 656-666 (1969)